Long-term behavior of precast, prestressed concrete sandwich panels reinforced with carbon-fiber-reinforced polymer shear grid

Mohamed K. Nafadi, Gregory Lucier, Tugce Sevil Yaman, Harry Gleich, and Sami Rizkalla

- This paper presents the results of an experimental program that studied the performance of full-scale precast, prestressed concrete sandwich panels reinforced with carbon-fiber-reinforced polymer shear grid and subjected to 2 million reverse-cyclic lateral load cycles with constant sustained axial load in place.
- Six sandwich panels were constructed with continuous insulation and a carbon-fiber-reinforced polymer grid shear transfer mechanism. Three of the panels were fabricated with expanded polystyrene foam insulation, and three panels were fabricated using sandblasted extruded polystyrene foam insulation.
- From each of the panel types, one specimen was tested to failure as a control. The other two specimens were subjected to fatigue testing and then tested to failure.
- The applied fatigue testing did not affect the ultimate performance of the panels and had a minimal effect on the composite action between the wythes.

PCI Journal (ISSN 0887-9672) V. 66, No. 5, September–October 2021.
PCI Journal is published bimonthly by the Precast/Prestressed Concrete Institute, 8770 W. Bryn Mawr Ave., Suite 1150, Chicago, IL 60631.

Precast concrete sandwich panels are typically used to construct high-performance, energy-efficient building envelopes. These panels typically consist of two concrete wythes separated by rigid foam insulation, such as expanded polystyrene (EPS) or extruded polystyrene (XPS). The panels are designed to resist floor loads as well as wind or seismic lateral loads while providing efficient insulation to the structure. They are often fabricated with heights over 45 ft (13.7 m) and widths up to 15 ft (4.6 m). Wythe thickness commonly ranges from 2 to 6 in. (50.8 to 152.4 mm), and overall panel thickness may be from 6 to over 12 in. (304.8 mm). Longitudinal prestressing is normally provided in both concrete wythes to control cracks.

Insulated concrete sandwich panels may be designed as fully composite, partially composite, or noncomposite. The degree of composite action highly depends on the type of shear connectors joining the concrete wythes. Typical shear connectors from early-generation precast concrete sandwich panels include steel-wire truss connectors, bent reinforcing bars, or solid zones of concrete penetrating the insulation wythe. Several published studies investigated the performance of such connectors and the associated degree of composite action of the panels.[1–6] Although increasing the composite action between the concrete wythes increases the structural efficiency of the panel, it can significantly reduce the overall thermal efficiency due to the thermal bridges produced through the shear connectors. Noncomposite panels then became more attractive due to their thermal benefits and architectural features; however, noncomposite panels exhib-

ited substantially reduced structural efficiency. Although the typical design for such panels assumes noncomposite action, test results from several studies indicate that significant shear transfer does develop between the concrete wythes, resulting in a partial composite action.[3–5]

Several studies investigated the use of fiber-reinforced polymer (FRP) shear connection grid as a mechanism for improving structural efficiency while avoiding the thermal bridges created by conventional means of shear transfer. Because FRP grid has very low thermal conductivity, the carbon grid can be used to connect the concrete wythes while maintaining the insulation of the panel. Several studies have also investigated the performance of glass-fiber-reinforced polymer (GFRP) shear connectors for insulated concrete sandwich panels.[7–12] These studies demonstrated that the use of GFRP increased the thermal performance of the panels compared with panels with steel or concrete connectors and maintained a high degree of composite action.

Frankl[13] and Frankl et al.[14] conducted an experimental program—including six full-scale precast, prestressed concrete sandwich panels—to investigate flexural behavior using carbon-fiber-reinforced polymers (CFRP) as a shear transfer mechanism. The study also investigated the effects of several parameters, such as the type of insulation, the presence of solid concrete zones, panel configuration, and shear grid reinforcement ratio. Test results indicated that the failure took place at levels well above factored design loads. The study also evaluated the degree of composite action for the tested panels and concluded that nearly 100% composite action can be achieved with CFRP grid shear connections. The study also demonstrated that a higher composite action percentage can be achieved using EPS insulation rather than XPS insulation. With either type of insulation, the use of CFRP shear grid can provide an effective shear transfer mechanism in precast, prestressed concrete sandwich wall panels.

Using Frankl's test results, an analytical study was carried out by Hassan et al.[15] to validate design guidelines proposed for precast, prestressed concrete sandwich panels reinforced with a CFRP grid. The study indicated good agreement between the experimentally measured strains at different load levels and those predicted using the proposed design guidelines. A simplified design chart was also proposed for panels with the same configuration as those tested experimentally to calculate the nominal flexural strength at different degrees of composite action.

Bunn,[16] Sopal,[17] and Hodicky et al.[18] conducted several experimental programs to study the CFRP grid and rigid foam insulation shear transfer mechanism and to investigate several parameters believed to influence shear flow strength. These studies developed equations to predict the shear flow strength provided by CFRP grid and rigid foam as affected by the tested parameters. It was concluded that the desired level of composite action could be achieved using CFRP grid with either EPS or XPS rigid foam insulation.

More recently, an experimental program conducted by Kazem et al.[19] evaluated the effect of sustained loading on the shear strength of precast concrete sandwich panels connected with CFRP and GFRP grids and using EPS and sandblasted XPS insulation. The experimental program comprised three different studies with a total of 26 test panels using different configurations of FRP grid and foam insulation. The research concluded that both CFRP and GFRP grid combined with EPS and XPS foam insulation can provide a suitable shear transfer mechanism for precast concrete sandwich panels under the effects of sustained load. In addition, the research findings demonstrated that the shear strength of the panels can be significantly increased by sandblasting the surface of the XPS foam due to the corresponding improvement of the bond between the foam and the concrete.

Another study, conducted by Olsen and Maguire,[20] examined the performance of GFRP connectors in precast concrete sandwich panels. The study included an experimental program to investigate the efficiency of several configurations of GFRP connectors along with the effects of other parameters, including the type of foam and the concrete-to-foam interface bond. The study concluded that the selected connectors provided reduced strength and stiffness with large wythe thicknesses and when debonded. In addition, the study developed a simplified model to evaluate the shear deformation behavior. A parametric study performed using the developed model concluded that a triangular distribution of connectors that has more connectors lumped near the ends exhibits higher structural efficiency and that the level of composite action generally increases when the number of shear connectors is increased.

Dutta et al.[21] conducted an experimental study to investigate the performance and efficiency of sandwich panels reinforced with new C-shaped GFRP pultruded channel shear connectors in terms of the level of composite action as well as the flexural strength. The shear connectors were configured in three forms: a continuous GFRP channel, discontinuous GFRP channel segments, and a control conventional steel truss. Test results indicated that panels with continuous GFRP channels performed the best in terms of flexural strength. The results also indicated that the level of composite action was about 50% for both continuous and discontinuous GFRP channels compared with 33% for the steel truss. These findings were verified by extensive finite element modeling, which also included a parametric study to investigate the effects of different parameters believed to affect the performance of sandwich panels reinforced with the new GFRP channels.[22] The finite element results also revealed that using circular openings in the GFRP channel web can be used to increase the efficiency of thermal insulation of the panel without affecting the structural performance.

Despite the extensive research conducted to study the behavior of precast, prestressed concrete sandwich panels reinforced with FRP shear grid, limited data are available regarding the long-term behavior of these members under the

effect of fatigue loading. This paper presents the results of an experimental program that was conducted to characterize the performance of full-scale precast, prestressed concrete sandwich panels reinforced with CFRP shear grid and subjected to 2 million reverse-cyclic lateral load cycles with constant sustained axial load in place.

Experimental program

A series of six panels were tested, including one group of three panels with EPS insulation and one group of three panels with sandblasted XPS insulation. One panel in each group of three was randomly selected as the control and was incrementally tested to failure under reverse-cyclic lateral loads. The remaining two panels in each group were subjected to 2 million fully reversed lateral load cycles at 45% of their design ultimate load before the failure test. Testing to 45% of the ultimate level of load for the fatigue cycles was chosen to represent the lateral loading resulting from the average typical wind speed that these panels would be subjected to over their life spans. A constant service-level eccentric axial load was in place for all tests, including the lateral fatigue cycles.

All panels were identical other than the insulation type. Each panel measured a nominal 8 in. (203.2 mm) thick, 4 ft (1.2 m) wide, and 20 ft (6.1 m) tall. **Figure 1** shows the three layers of the typical cross section of all panels. The panel configuration included the following:

- 2 in. (50.8 mm) prestressed concrete outer wythe
- 4 in. (101.6 mm) center layer of EPS or sandblasted XPS foam insulation
- 2 in. prestressed concrete inner wythe

The test specimens were labeled as follows:

- EPS1: first specimen with EPS insulation tested to failure
- EPS2: second specimen with EPS insulation subjected to fatigue cycles before the failure test
- EPS3: third specimen with EPS insulation subjected to fatigue cycles before the failure test

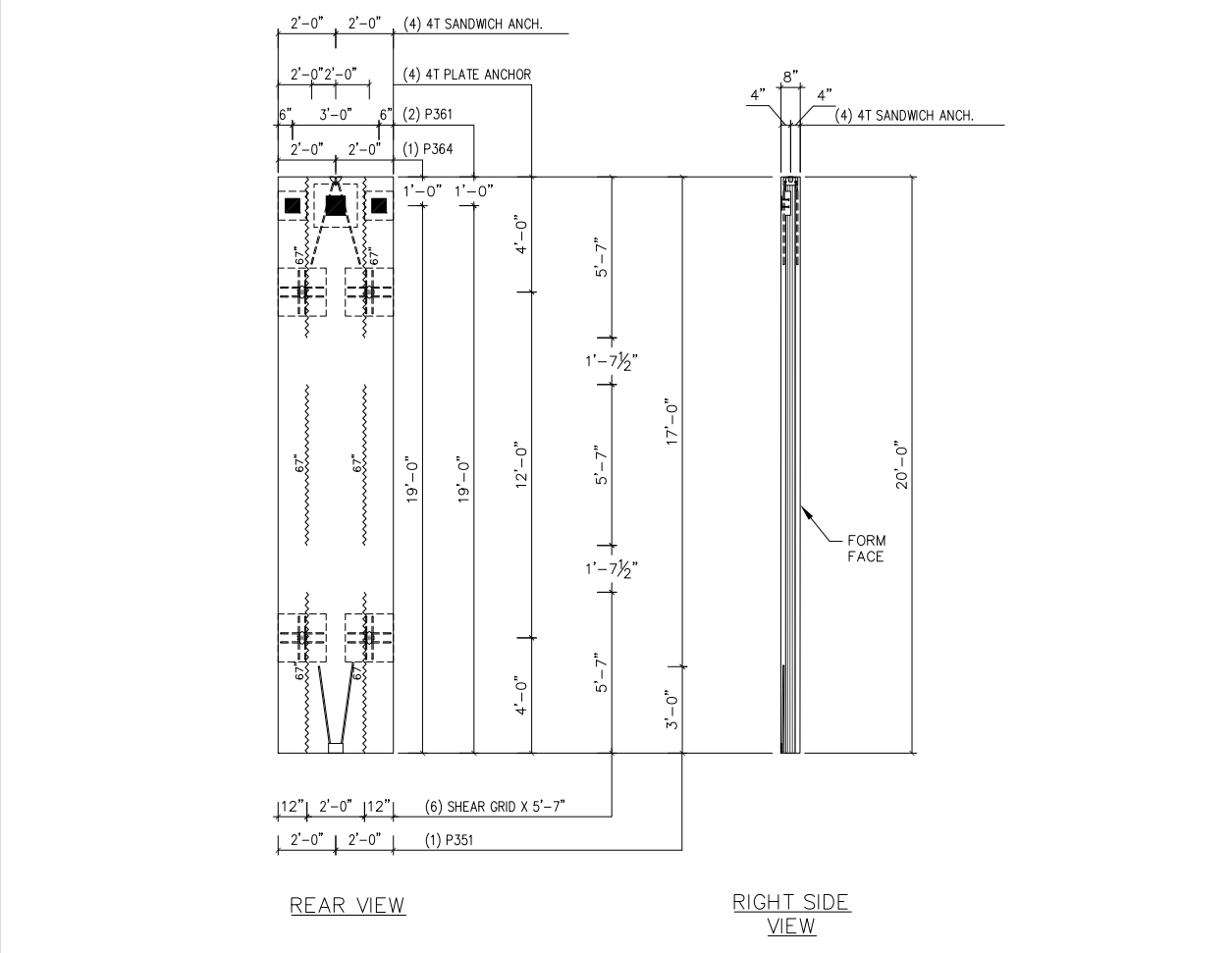

Figure 1. Specimen cross section from producer shop tickets. Note: 1″ = 1 in. = 25.4 mm; 1′ = 1 ft = 0.305 m.

- XPS1: first specimen with sandblasted XPS insulation tested to failure
- XPS2: second specimen with sandblasted XPS insulation subjected to fatigue cycles before the failure test
- XPS3: third specimen with sandblasted XPS insulation subjected to fatigue cycles before the failure test

Each concrete wythe was prestressed longitudinally with two $\frac{3}{8}$ in. (9.525 mm) diameter strands in addition to one layer of welded-wire reinforcement with W3.5 wires spaced at 8 in. (203.2 mm) in the transverse direction. CFRP grid was provided between the wythes to transfer shear across the rigid insulation. Two strips of the grid were placed parallel to the long axis of each panel at the locations shown in **Fig. 2**. A small additional strip of CFRP grid was placed in the transverse panel direction to reinforce the region surrounding the lifting points for a total of 36 ft (11 m) of CFRP grid in each panel. The installed CFRP grids were orthogonal and cut at a 45-degree angle to develop truss action. The rigid foam insulation was thinned in areas surrounding embedded connections and lifting points; however, the insulation was continuous from end to end and from side to side. Care was taken in the experimental design to ensure that the testing setup itself did not artificially enhance the connection between inner and outer wythes.

Construction of wall panels

The panels were cast flat in long-line production forms. Fabrication began by placing formwork, stressing strands, and laying reinforcement for the outer wythe of concrete. After casting a 2 in. (50.8 mm) layer of concrete for the outer wythe, prefabricated foam insulation and CFRP grid assemblies were placed on top, and CFRP grid was pushed into the wet concrete wythe beneath. With the CFRP grid projecting up from the insulation, the top wythe welded-wire reinforcement was placed. The top wythe concrete was cast, and embedded plates for connections and lifting devices were set. **Figure 3** shows typical photographs of the panels during construction.

The specified concrete strength was 5000 psi (34.5 MPa) and the average compressive strength of the wall panels at time of testing was 8500 psi (58.6 MPa), as determined by compression tests of three 4 × 8 in. (101.6 × 203.2 mm) cylinders cast with the test panels.

Design loads and loading sequence

The panels were designed for a maximum lateral wind pressure of 42.5 lb/ft^2 (2.03 kPa) due to suction in combination with a service-level axial load of 4 kip (17.8 kN). The lateral wind loadings were determined according to the design wind pressures specified in American Society of Civil Engineers' ASCE/SEI 7-16[23] chapter 30, assuming a basic wind speed of 150 mph (240 km/hr), building classification III, and exposure category B. The tested panels were designed per the standard procedures of the shear grid manufacturer, as documented in International Code Council Evaluation Service (ICC-ES) report ESR-2953,[24] which includes shear flow and shear modulus of the grid connectors. The axial load was applied through a steel corbel at the top of the panel having an eccentricity of 4 in. (101.6 mm) from the innermost surface of the inner wythe. Lateral loads were applied in four-point bending, with the panel supported laterally at the top and bottom and loaded equally at the quarter and three-quarters heights. The quarter and three-quarters heights did not exactly match the quarter and three-quarters spans because the top support was located

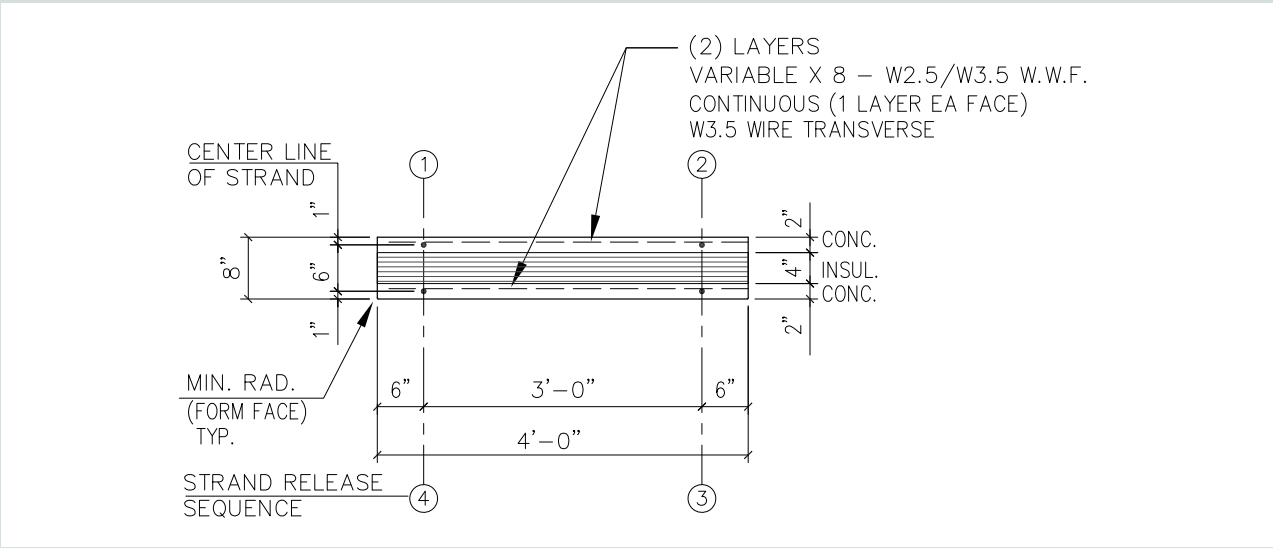

Figure 2. Specimen plan and profile from producer shop tickets. Note: CONC. = concrete; EA = each; INSUL. = insulation; MIN. = minimum; RAD. = radius; TYP. = typical; W.W.F. = welded-wire reinforcement. 1″ = 1 in. = 25.4 mm; 1′ = 1 ft = 0.305 m.

Forms with outer wythe reinforcement installed

Foam core with carbon-fiber-reinforced polymer grid installed after casting the outer wythe

Figure 3. Typical views of panels during fabrication.

below the top of the panel, which is common for typical roof detailing. Quarter-height lateral loading was chosen so that the moment and shear distributions of the applied lateral test loads would closely mimic those of uniformly distributed wind pressure.

One EPS panel and one sandblasted XPS panel were randomly selected as the control specimens and were incrementally tested to failure under reverse-cyclic lateral loads. The axial load was applied with hydraulic cylinders before lateral loading and was held constant using nitrogen-charged hydraulic accumulators during the entire test. Lateral loads were applied incrementally in both directions, pushing and pulling, in 1000 lb (4.45 kN) increments (500 lb [2.22 kN] per loading jack). **Table 1** summarizes the loading scheme. One load cycle was considered as taking the panel from zero lateral load to the specified lateral load level in both directions.

Two EPS panels and two sandblasted XPS panels were each subjected to 2 million reverse-cyclic lateral load cycles before failure testing (Table 1). Cycles were applied at a rate of approximately 1 Hz, for a total cycling time of approximately 23 days per panel. A constant axial load was applied to the panels during all fatigue loading. Each fatigue cycle induced lateral loading in the positive and negative directions to a selected lateral load corresponding to 45% of the design

Table 1. Loading sequence for all static tests to failure

Step	Loads on panel			
	Total applied lateral load, lb	Load per actuator, lb	Equivalent uniform pressure on panel, lb/ft²	Axial load, lb
1	±1000	±500	±12.5	4000
2	±2000	±1000	±25	4000
3	±3000	±1500	±37.5	4000
4	±4000	±2000	±50	4000
5	Continue increasing each increment by ±1000 lb to failure	(Total load)/2	(Total load)/20 ft/4 ft	4000

Note: 1 ft = 0.305 m; 1 lb = 0.00445 kN; 1 lb/ft² = 0.048 kPa.

ultimate load. Such value was selected to represent the typical service-level wind load that would be expected during average service (that is, the average wind speed over the life of the panel). This load level was equivalent to 19.1 lb/ft^2 (0.91 kPa), 1530 lb (6.8 kN) of the total lateral load, and 765 lb (3.4 kN) of the lateral load per load point. After fatigue testing, each panel was subjected to the incremental static test to failure as previously described.

Test setup

The test setup was designed to enable cycling two panels simultaneously but independently. Two identical setups were fabricated side by side under the same supporting frame (**Fig. 4** and **5**). All panels were supported at the bottom on a pin connection that restrained translation in all directions but allowed rotation. Only the inner wythe was connected to the lower connection to avoid artificially enhancing the connection between wythes. All panels were supported at the top on a slotted roller that allowed vertical translation and rotation but prevented lateral translation. The top lateral support (and axial load connection) was attached only to the inner wythe, as would be common in practice for the detailing of a typical panel.

Two matching hydraulic actuators were used to apply tension and compression loads in the lateral direction. The actuators were always configured to produce matching loads, regardless of actuator stroke or panel deflection. Each actuator was attached to the panel using two 4 ft (1.2 m) long square loading tubes, one on each surface of the panel. The loading tubes were bolted together through substantially oversized holes in the panel to allow application of lateral loads in either direction without artificially connecting the wythes. The loading tubes were separated from the panel surface by a thick neoprene pad on each wythe to avoid unintentionally restraining the panel with the loading system. Axial load was applied with a hydraulic jack to the top of the panel through a steel corbel welded to the embedded plate. The axial load was applied and regulated using accumulators charged with nitrogen in the axial load hydraulic circuit. This configura-

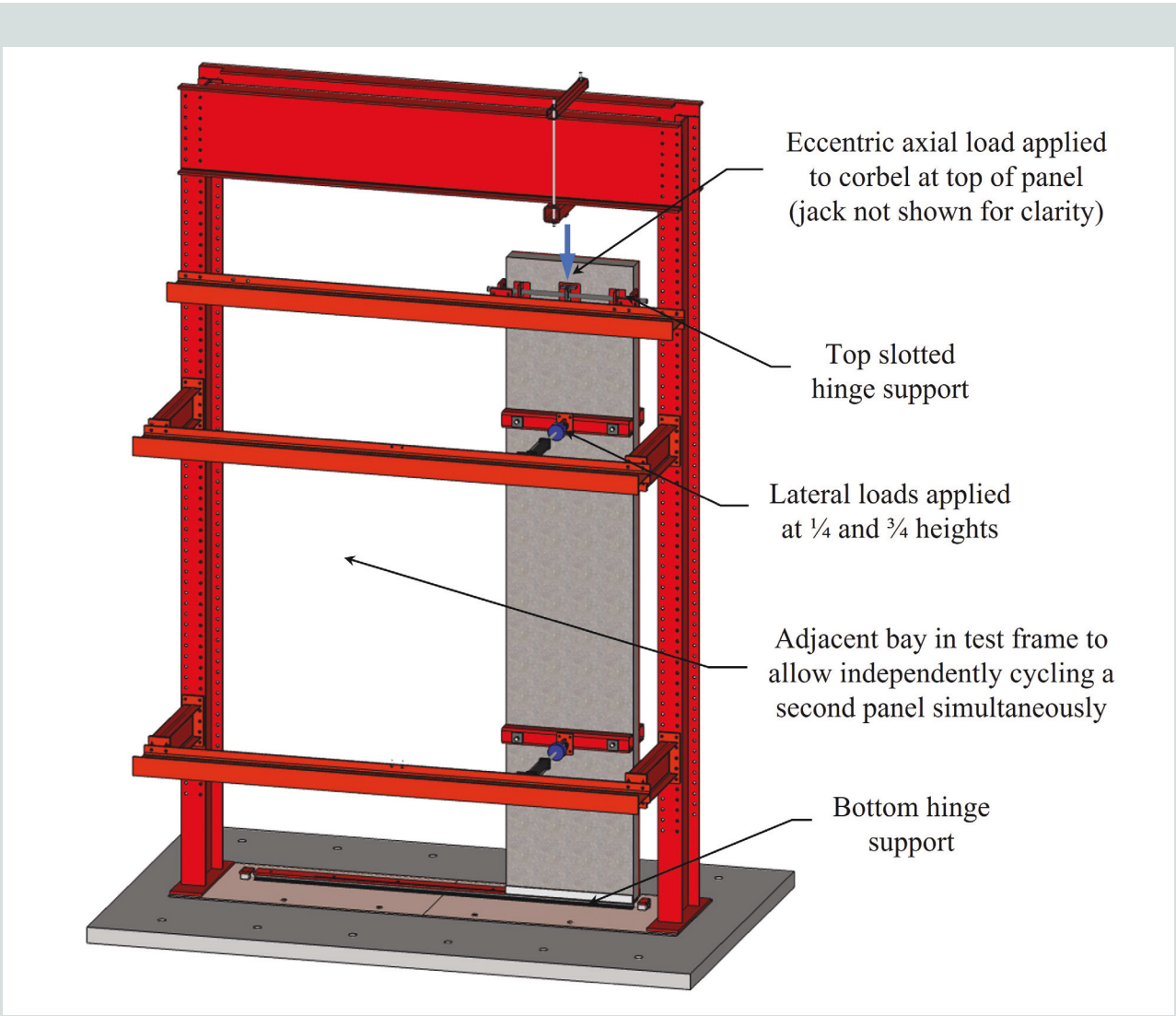

Figure 4. Schematic of the test setup, view of inner wythe.

Test setup with one panel

Test setup with two panels

Figure 5. Views of the test setup.

tion allowed the axial load to remain virtually constant as the panel deformed laterally. The corbel was specially configured to avoid interfering with the lateral supports.

Instrumentation

Various instruments were used during testing to monitor panel behavior. All instruments were connected to an electronic data acquisition system, which recorded data at a sample rate of 1 Hz during static loading and at 10 Hz for selected intervals during cyclic loading. **Figure 6** shows the instrumentation layout and sign convention for applied loads and measured deflections.

Various load cells were used to measure the applied axial load as well as the lateral loads. Axial load was maintained by applying constant hydraulic pressure to a calibrated hydraulic jack. The axial load was considered positive when acting to place the inner wythe in compression (that is, the positive axial load acts vertically downward). One load cell was incorporated into the body of each lateral load jack. These load cells were used to continuously monitor the applied lateral load.

For the test setup as configured, extension in the lateral actuators created positive loads while the tension in the actuators was considered negative load.

Potentiometers were used to monitor the lateral deflections of the panel throughout each test at different locations (Fig. 6). All deflection data presented in subsequent sections are plotted according to the given sign convention and are adjusted to eliminate the effects of support motion. Lateral deflections were considered positive when they acted to place the inner wythe in compression (that is, positive lateral deflection is the panel moving outward).

To characterize the degree of composite action of the panel, two groups of four strain gauges each were attached to the side surfaces of the two concrete wythes. One group of four gauges was attached at midheight, and the other group of four gauges was attached at a location 1 ft (0.305 m) below the three-quarters height (1 ft below the upper load point). All gauges were centered $^{7}/_{16}$ in. (11.1 mm) from the nearest wythe surface or wythe-foam interface. Figure 7 shows the groups of bonded strain gauges.

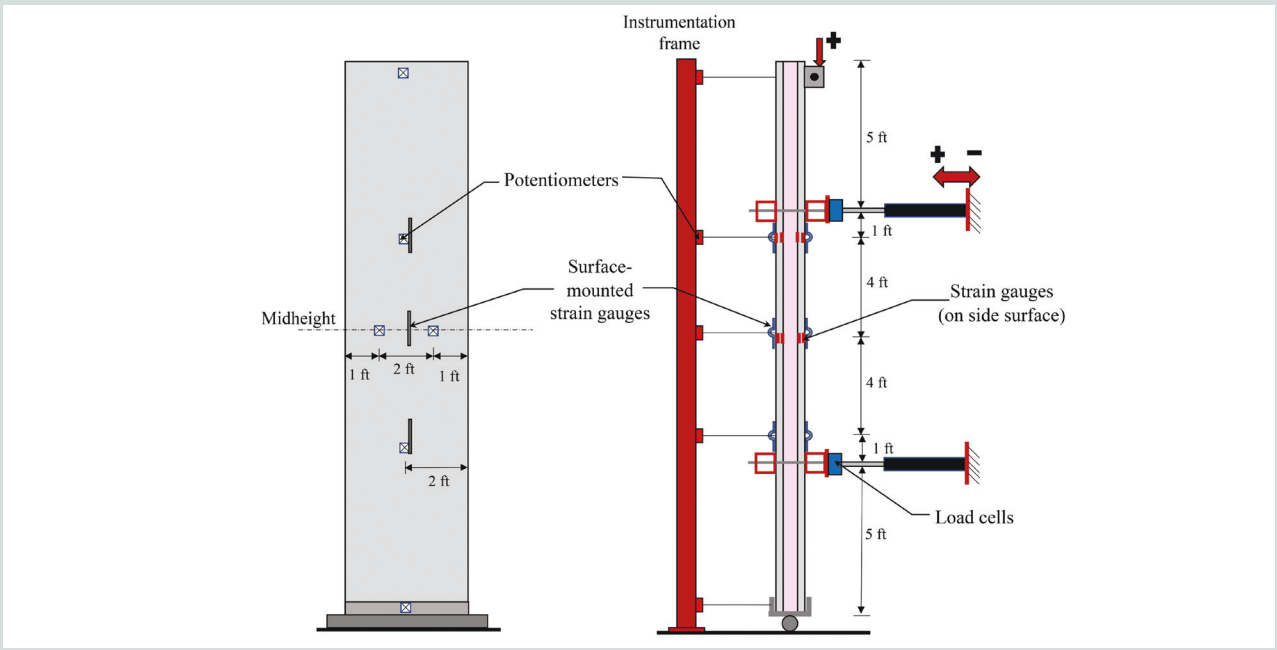

Figure 6. Instrumentation layout and sign convention for applied loads and measured deflections. Note: 1 ft = 0.305 m.

In addition to the strain gauges, six reusable surface-mounted strain gauges, referred to as pi gauges, were used to measure the flexural strain at the concrete surface of the panel. Three gauges were installed on the inner panel surface and three gauges on the outer panel surface. **Figure 7** shows the outer-face pi gauges on a selected panel. All bonded strain gauges and pi gauges were attached to the panel after fatigue testing to avoid fatiguing the gauges themselves. All measured strains were considered positive in tension and negative in compression.

Results and discussion

Table 2 summarizes the test results. For all tests, the negative segment of a given lateral load cycle (the segment with the inner wythe in tension) was completed before the positive segment of that cycle was attempted. Due to the effects of the eccentric axial load, the bending moment created in the panel during the positive segment of each cycle was greater than the moment created by the same lateral load on the negative segment. All four panels subjected to fatigue loading survived 2 million lateral load cycles without any visible signs of degradation. These four panels were then tested to failure using the incremental static loading procedure outlined in the previous section. A constant 4 kip (17.8 kN) eccentric axial load was applied to the corbel at the top of each panel during all phases of loading, including fatigue cycles. The axial load application was regulated to remain constant even as the panel deformed under lateral load. The equivalent lateral design wind pressure was 42.5 lb/ft^2 (2.03 kPa). All six panels sustained applied lateral loads well in excess of their design values.

The results indicate that the tested EPS panels all failed when the applied lateral load was greater than or equal to 100 lb/ft^2 (4.79 kPa). In this group of three panels, one of the two fatigued panels outperformed the control panel in terms of ultimate load: EPS2 achieved 112.5 lb/ft^2 (5.39 kPa) compared with 100 lb/ft^2 for EPS1. It is unlikely that the fatigue cycles enhanced the panel performance in any way, and it is also unlikely that the small increase in concrete compressive strength (due to panel aging) that probably occurred during the fatigue cycles improved ultimate failure performance. At 100 lb/ft^2 of applied lateral load (with 4 kip [17.8 kN] of axial load in place), the panels exceeded their design load of 42.5 lb/ft^2 (2.03 kPa) by a factor of 2.35.

The tested XPS panels all failed at the equivalent of 175 lb/ft^2 (8.38 kPa) of applied lateral pressure, which was higher than that achieved by the EPS panels. This can be attributed to the fact that sandblasted XPS has greater bond strength, shear strength, and stiffness than EPS, evidenced by a nominal shear flow design value of 450 lb/in. (50.8 N/m) for XPS and CFRP grid compared with 270 lb/in. (30.5 N/m) for EPS and CFRP grid. The XPS panels achieved an ultimate lateral load that was more than four times their 42.5 lb/ft^2 (2.03 kPa) design load. All tested panels were designed using the standard prescribed design methods of the CFRP grid manufacturer, so these high overstrengths against shear transfer mechanism failure would also be typical of production panels. Part of the excess capacity can likely be attributed to measured concrete strength exceeding that specified by design (8500 psi [58.6 MPa] compared with 5000 psi [34.5 MPa], respectively); however, the effect of modestly increased concrete strength on panel capacity is likely minimal. Both EPS and XPS panels exceeded their design levels by ratios greater than the increase of nominal flexural or shear strength due to the increased concrete compressive strength. The selected

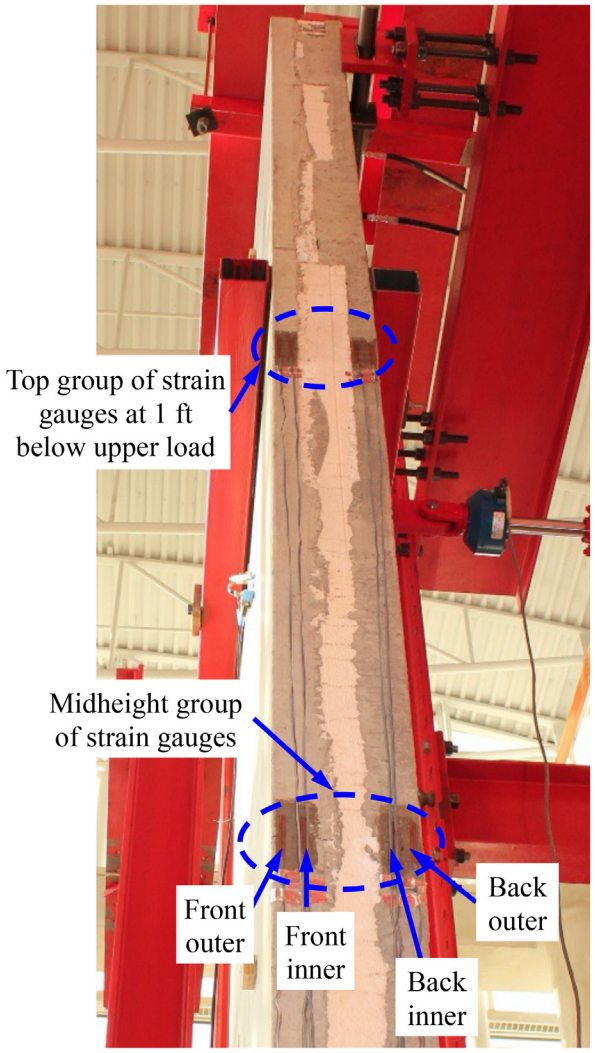

Strain gauges

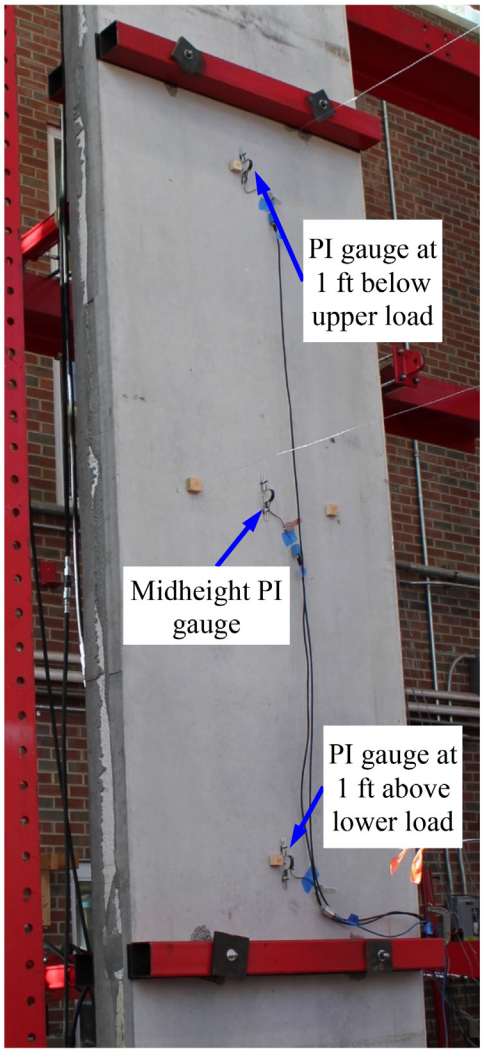

Surface-mounted strain gauges (pi gauges)

Figure 7. Photographs of instrumentation. Note: 1 ft = 0.305 m.

fatigue regimen did not seem to negatively affect the ultimate performance of the panels in any way. It is noted that the applied fatigue loading of 45% of the design ultimate load ended up being about 19% and 11% of the actual ultimate load of the EPS and XPS panels, respectively, due to the panel overstrength. These levels of overstrength were achieved with standard design methods and therefore would be typical of production panels designed with the same methods.

Cracking patterns and failure modes

Observed cracking in all panels primarily took the form of horizontal flexure cracking in the zone between the load points. **Figure 8** shows examples of typically observed cracks, failure modes, and a typical CFRP grid failure. Critical cracks often developed at or near failure at the lower loading point. This can be attributed to the fact that the upper support was about 1 ft (0.305 m) below the top face of the panel, and the locations of the applied loads were not fully symmetric with respect to the supports (Fig. 6). Hence, the location of the maximum moment was consistently shifted to the lower loading point, whether the load was applied in pulling or pushing directions. All panels were visually uncracked at the start of failure testing, including panels that had been subjected to the 2 million fatigue cycles. The following sections describe the cracking pattern and failure mode for each tested panel.

EPS1-control Horizontal cracks were first observed on the inner wythe of the EPS control panel during the pulling segment of a total applied load cycle of 8000 lb (35.6 kN). The test was terminated because the panel could not sustain this load level and continued to displace laterally under the

Table 2. Summary of results for all panels

Panel	Total ultimate applied lateral load, lb	Total ultimate equivalent uniform pressure, lb/ft²	Failure cycle	Failure mode
EPS1-control	8000 (pull)	100	4000 lb/jack cycle (pull)	Global flexure failure accompanied by loss of shear transfer after reaching 4000 lb/jack pulling (did not sustain this level).
EPS2-fatigued	9000 (pull)	112.5	4500 lb/jack cycle (push)	Global flexure and shear failure at lower lateral load point with loss of shear transfer. Survived 4500 lb/jack pulling. Failed at 4000 lb/jack while pushing towards 4500 lb/jack on subsequent segment.
EPS3-fatigued	8000 (push)	100	4000 lb/jack cycle (push)	Global flexure and shear failure at lower lateral load point with loss of shear transfer. Survived 4000 lb/jack pulling. Reached 4000 lb/jack pushing but could not sustain this load.
XPS1-control	14,000 (pull)	175	7000 lb/jack cycle (pull)	Global flexural failure after reaching 7000 lb/jack pulling. Did not sustain this load level.
XPS2-fatigued	14,000 (push)	175	7000 lb/jack cycle (push)	Extensive global flexural behavior followed by ultimate flexure and shear crack at the lower load point. Reached 7000 lb/jack pushing but did not sustain this level.
XPS3-fatigued	14,000 (pull)	175	7000 lb/jack cycle (push)	Global flexural failure at the lower lateral load point. Sustained 7000 lb/jack pulling, failed at 6500 lb/jack while pushing towards 7000 lb/jack on subsequent segment.

Note: EPS1-control = first specimen with expanded polystyrene insulation tested to failure; EPS2-fatigued = second specimen with expanded polystyrene insulation subjected to fatigue cycles before the failure test; EPS3-fatigued = third specimen with expanded polystyrene insulation subjected to fatigue cycles before the failure test; XPS1-control = first specimen with sandblasted extruded polystyrene insulation tested to failure; XPS2-fatigued = second specimen with sandblasted extruded polystyrene insulation subjected to fatigue cycles before the failure test; XPS3-fatigued = third specimen with sandblasted extruded polystyrene insulation subjected to fatigue cycles before the failure test. 1 lb = 0.00445 kN; 1 lb/ft² = 0.048 kPa.

constant applied load. Significant relative displacement was observed at the interface between the inner concrete wythe and foam core at and after failure. This behavior suggests that the failure took place due to a loss of composite action between the wythes that led to a global flexure failure.

EPS2-fatigued Similar to EPS1, no cracks were observed on EPS2 before failure. As the failure developed, a large flexure crack appeared underneath the lower loading tube. This crack was accompanied by concrete crushing on the opposite face. The panel sustained a total applied load of 9000 lb (40 kN) on the pulling segment in the cycle segment before failure. A global flexure and shear failure due to loss of composite action then took place at the lower lateral load point at a total applied load of 8000 lb (35.6 kN) while pushing toward 9000 lb on the subsequent pushing segment.

EPS3-fatigued EPS3 behaved in a similar fashion to EPS2, as expected. The panel remained visually uncracked until just before failure. Horizontal cracks developed at the lower load point (Fig. 8). A secondary horizontal crack developed between the lower lateral load point and the support, likely due to a partial loss of composite action at failure. Failure in the shear transfer mechanism then triggered an immediate global flexure and shear failure that took place at the lower lateral load point at a total applied load of 8000 lb (35.6 kN) in the pushing segment, which the panel reached but could not sustain.

XPS1-control Panel XPS1 demonstrated significant global flexural action before failure, including extensive horizontal cracking between the load points and below the lower load point. Horizontal cracks were obvious on the inner and outer wythes at the cycle of a total applied load of 8000 lb (35.6 kN). Horizontal cracks continued to grow in width and to increase in number before failure. Unlike the EPS panels, the XPS1 panel was able to continue resisting total applied loads up to 14,000 lb (62.2 kN) at a pulling segment, at which a global flexural failure took place.

XPS2-fatigued Cracking in XPS2 progressed in much the same way as for XPS1. Horizontal cracks developed and spread on both faces as loading increments increased. The panel exhibited extensive global flexural behavior followed by an ultimate flexure and shear crack at the lower load point at a total applied load of 14,000 lb (62.2 kN) in the pushing segment, which the panel reached but could not sustain.

XPS3-fatigued XPS3 behaved in much the same way as XPS2, as expected. The failure mode was due to a large flex-

Third test specimen with expanded polystyrene insulation (EPS3)

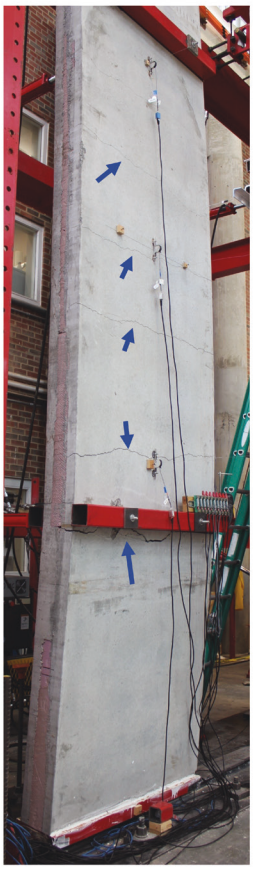

Third test specimen with sandblasted extruded polystyrene insulation (XPS3)

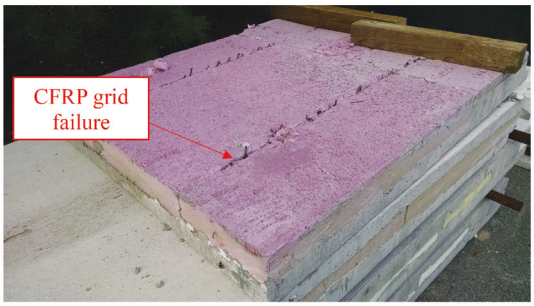

Typical CFRP grid failure

Figure 8. Cracking pattern and failure mode of test specimens. Note: CFRP = carbon-fiber-reinforced polymer.

ure and shear crack at the lower load point (Fig. 8). The panel could sustain up to a total applied load of 14,000 lb (62.2 kN) on the pulling segment, followed by a global flexural failure at the lower lateral load point at 13,000 lb (57.8 kN) of total applied load while pushing toward the same 14,000 lb target.

Measured lateral deflections

Figures 9 and **10** compare the lateral deflections measured at the midheights of the EPS and XPS panels, respectively. For

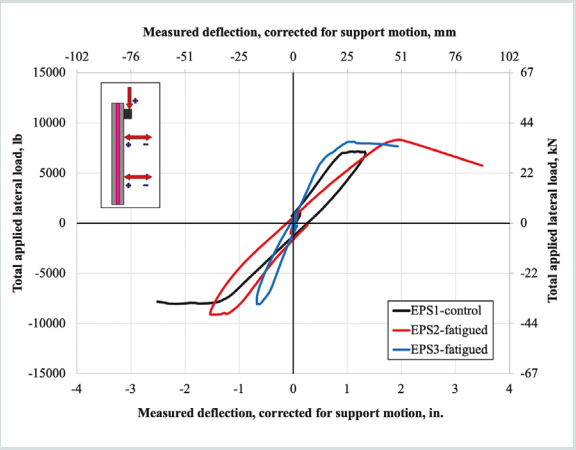

Figure 9. Measured lateral deflections at midheight for the EPS panels. Note: Only the first and last cycles are shown for better clarity. EPS = expanded polystyrene; EPS1-control = first specimen with expanded polystyrene insulation tested to failure; EPS2-fatigued = second specimen with expanded polystyrene insulation subjected to fatigue cycles before the failure test; EPS3-fatigued = third specimen with expanded polystyrene insulation subjected to fatigue cycles before the failure test.

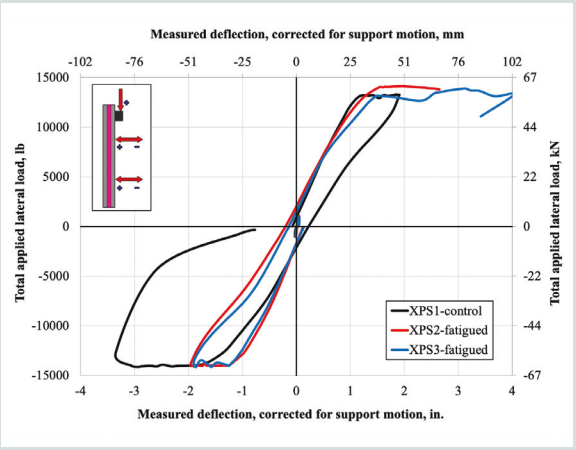

Figure 10. Measured lateral deflections at midheight for the sandblasted XPS panels. Note: Only the first and last cycles are shown for better clarity. XPS = extruded polystyrene; XPS1-control = first specimen with sandblasted XPS insulation tested to failure; XPS2-fatigued = second specimen with sandblasted XPS insulation subjected to fatigue cycles before the failure test; XPS3-fatigued = third specimen with sandblasted XPS insulation subjected to fatigue cycles before the failure test.

better clarity, the figures show only the first and last cycles. The overall performance of all three panels was quite similar. The initial stiffness of control panel EPS1 and fatigued panel EPS2 are quite similar. Interestingly, the initial stiffness of fatigued panel EPS3 slightly exceeds that of EPS1 and EPS2, likely due to random variations in the manufacturing process. In addition, the residual deflections (hysteresis) observed during the static cycles of EPS3 are relatively less than those

from equivalent cycles for EPS1 and EPS2. This finding implies that panel EPS3 had a better bond between concrete and foam than did panels EPS1 and EPS2. It is not reasonable to conclude that fatigue cycling enhanced the EPS3 bond in any way, so it is assumed that this better bond was due to natural variability in the manufacturing process. Panels EPS1, EPS2, and EPS3 were manufactured at the same time from the same material inputs, and no obvious differences in the production of these three panels were observed. Therefore, it is concluded that the fatigue cycles did not influence the final load-deflection behavior of the EPS panels.

Figure 10 shows the measured lateral deflections at the midheights of the XPS panels. The behaviors of the control panel XPS1 and the fatigued panels XPS2 and XPS3 could not be distinguished from this plot. The overall behaviors appeared to be identical for all practical purposes, and the initial stiffness matched across the three tests. It is concluded that the fatigue cycles did not affect the final load-deflection behavior of the tested XPS panels.

Measured strains

Two groups of four strain gauges each were used to monitor the strains across the panel thickness at midheight and at 1 ft (0.305 m) below the upper load point. The measured strains were then used to plot the strain profiles across the thickness for each panel at different load levels to characterize the degree of composite action.

Figure 11 shows strain profiles plotted for each panel at a selected load level, where a total applied lateral load of 3400 lb (15.1 kN) was pushing the panel outward at 1 ft (0.305 m) below the upper load and at midheight of each panel. The load level represents an equivalent uniform pressure on the panel of 42.5 lb/ft^2 (2.03 kPa), which is the design lateral wind pressure. Despite the small values of the measured strains, which were close to the accuracy of the instrumentation, the recorded strains at the outer and inner surfaces were clearly in opposite directions as the inner wythe was in compression while the outer wythe was in tension. The results indicate

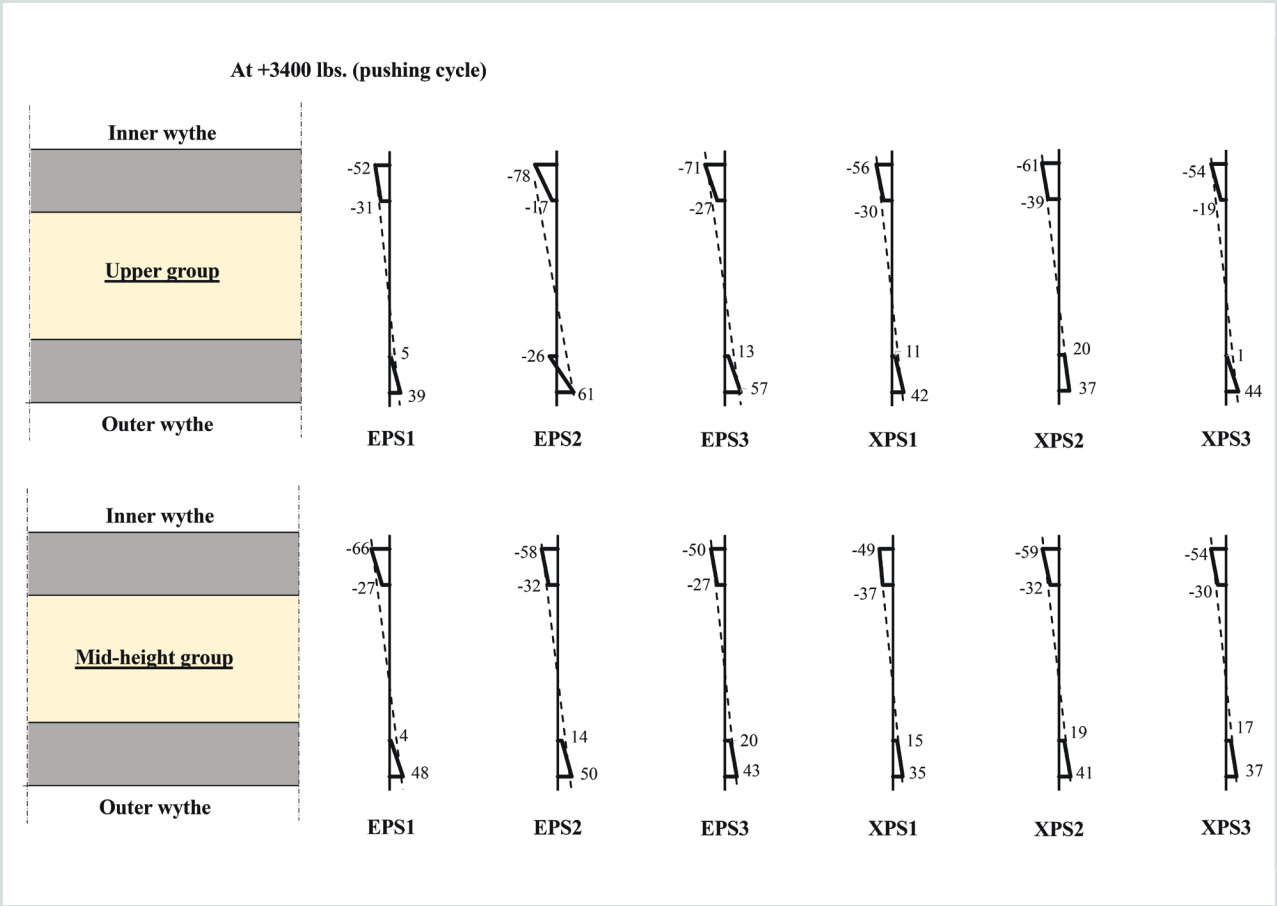

Figure 11. Measured strains across the panel thickness at total applied load of 3400 lb (pushing segment) at upper and midheight groups of strain gauges. Note: Measured strains are in microstrain. EPS1 = first specimen with expanded polystyrene insulation tested to failure; EPS2 = second specimen with expanded polystyrene insulation subjected to fatigue cycles before the failure test; EPS3 = third specimen with expanded polystyrene insulation subjected to fatigue cycles before the failure test; XPS1 = first specimen with sandblasted extruded polystyrene insulation tested to failure; XPS2 = second specimen with sandblasted extruded polystyrene insulation subjected to fatigue cycles before the failure test; XPS3 = third specimen with sandblasted extruded polystyrene insulation subjected to fatigue cycles before the failure test. 1 lb = 0.00445 kN.

that the strain profiles for all of the panels were nearly linear except one location at the upper gauge group in panel EPS2, where each wythe appeared to act independently. These results suggest that all of the panels were generally able to exhibit a relatively high degree of composite action up to the design load. Furthermore, it could be concluded that the applied fatigue cycling before the failure test had a minimal effect on the composite action between the wythes.

These results indicate that in the EPS panels, a loss of composite action likely triggered flexural failure and in the sandblasted XPS panels, a loss of composite action was likely triggered by flexural failure. Although the findings of Frankl et al.[14] indicate that a higher degree of composite action can be achieved using EPS insulation than standard XPS insulation, these results indicate that the sandblasted XPS panels could maintain a higher degree of composite action up to failure compared with EPS panels. This can be mainly attributed to the beneficial effect from sandblasting the surface of the XPS foam, which is expected to improve the bond between the concrete wythes and the foam and, consequently, increase the degree of composite action and overall flexural and shear strengths of the panels.

Figure 12 shows an example of measured strains at both the inner and outer concrete faces for panel EPS3. The measured strains were generally small in value and symmetrical with respect to the vertical axis. The load versus strain behavior was fairly linear up to the failure at all locations except near the lower loading point at both the inner and outer faces, where flexural and shear cracks initiated before failure. This behavior is consistent with the visual observations during the test, which did not reveal any cracks until just before the failure.

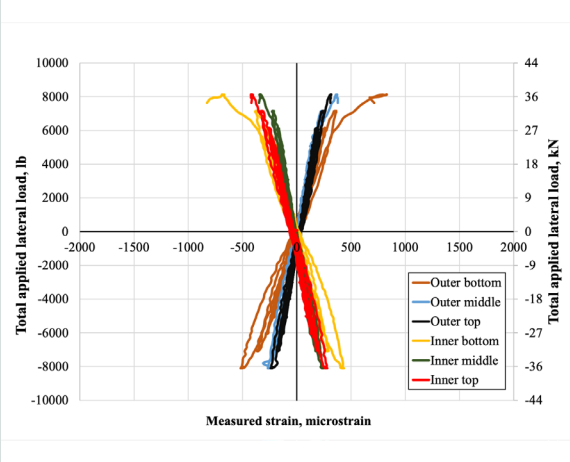

Figure 12. Measured concrete strains at inner and outer faces of panel EPS3. Note: EPS3 = third specimen with expanded polystyrene insulation subjected to fatigue cycles before the failure test. 1 lb = 0.00445 kN.

Conclusion

This paper documents testing of six 20 × 4 ft (6.1 × 1.2 m) precast, prestressed concrete sandwich panels constructed with continuous insulation and a CFRP grid shear transfer mechanism. All panels were identical except for foam type, and all panels were cast together on the same long-line prestressing bed. Three of the six panels were fabricated with EPS foam insulation, and the remaining three panels were fabricated using sandblasted XPS foam insulation. For each group of three panels, one was randomly selected and tested to failure as a control and two others were each subjected to 2 million lateral load cycles equivalent to 45% of their ultimate lateral design capacity, in combination with a service-level axial load. After fatigue testing, all panels were tested to failure. The conclusions are as follows:

- All tested panels were designed with standard commercial methods using the manufacturer's recommended values for shear flow, and all sustained applied lateral loads well in excess of their design values. The EPS panels all failed when the applied lateral load was greater than or equal to 100 lb/ft^2 (4.79 kPa), which is 2.35 times their design load of 42.5 lb/ft^2 (2.03 kPa). The tested sandblasted XPS panels failed at the equivalent of 175 lb/ft^2 (8.38 kPa) of applied lateral pressure, equivalent to over 4.0 times their design ultimate load of 42.5 lb/ft^2.
- All four panels subjected to fatigue survived 2 million lateral load cycles without any visible signs of degradation. For the EPS panels, the two fatigued panels slightly outperformed the control panel in terms of ultimate load (EPS2 achieved 112.5 lb/ft^2 [5.39 kPa]) and initial stiffness (EPS3 exhibited a greater initial stiffness). Therefore, it is concluded that the effects of fatigue at the selected levels on the ultimate load-deflection performance are less significant than are the effects of variability in the manufacturing process. For the XPS panels, the load-deflection behaviors of the three panels were indistinguishable up to failure, indicating a high level of consistency in the manufacturing process and foam-to-concrete bond for these panels.
- All panels demonstrated a high degree of composite action through load levels well in excess of their 42.5 lb/ft^2 (2.03 kPa) design load; however, composite action was lost at failure. It is likely that a loss of composite action triggered failure in the EPS panels and that global failure triggered loss of composite action in the sandblasted XPS panels. The sandblasted XPS panels showed a higher level of composite action than the EPS panels, as would be expected by the larger stiffness of XPS compared with EPS and the strong bonding characteristics of sandblasted XPS. This behavior can be attributed to the beneficial effects of sandblasting the surface of the XPS foam, which is expected to improve the bond between the concrete wythes and the foam and consequently increase the degree of composite action and the overall flexural and shear strengths of the panels.

Acknowledgments

The authors would like to acknowledge AltusGroup for sponsoring these tests and for designing, producing, and transporting the test panels. The authors are also grateful to Metromont Corp. and its crews in Charlotte, N.C., for fabricating the test specimens. In addition, the authors would like to thank the staff at the Constructed Facilities Laboratory at North Carolina State University for their help throughout the experimental program. Finally, the authors would like to acknowledge Hamid Kazem, the former postdoctoral fellow at North Carolina State University, for his assistance with the experimental program.

References

1. Gleich, H. 2007. "New Carbon Fiber Reinforcement Advances Sandwich Wall Panels." *Structure Magazine* (April): 61–63.

2. PCI Committee on Precast Sandwich Wall Panels. 1997. "State of the Art of Precast/Prestressed Sandwich Wall Panels." *PCI Journal* 42 (2): 92–134.

3. Pessiki, S., and A. Mlynarczyk. 2003. "Experimental Evaluation of Composite Behavior of Precast Concrete Sandwich Wall Panels." *PCI Journal* 48 (2): 54–71.

4. Bush, T. D., and G. L. Stine. 1994. "Flexural Behavior of Composite Prestressed Sandwich Panels." *PCI Journal* 39 (2): 112–121.

5. Lee, B., and S. Pessiki. 2007. "Design and Analysis of Precast, Prestressed Concrete Three-Wythe Sandwich Wall Panels." *PCI Journal* 52 (4): 70–83.

6. Lee, B., and S. Pessiki. 2008. "Experimental Evaluation of Precast, Prestressed Concrete, Three-Wythe Sandwich Wall Panels." *PCI Journal* 53 (2): 95–115.

7. Salmon, D. C., A. Einea, M. K. Tadros, and T. D. Culp. 1997. "Full Scale Testing of Precast Concrete Sandwich Panels." *ACI Structural Journal* 94 (4): 354–362.

8. Lameiras, R., J. Barros, I. B. Valente, and M. Azenha. 2013. "Development of Sandwich Panels Combining Fibre Reinforced Concrete Layers and Fibre Reinforced Polymer Connectors. Part I: Conception and Pull-Out Tests." *Composite Structures* 105: 446–459.

9. Lameiras, R., J. Barros, M. Azenha, and I. B. Valente. 2013. "Development of Sandwich Panels Combining Fibre Reinforced Concrete Layers and Fibre Reinforced Polymer Connectors. Part II: Evaluation of Mechanical Behaviour." *Composite Structures* 105: 460–470.

10. Maximos, H. N., W. A. Pong, M. K. Tadros, and L. D. Martin. 2007. "Behavior and Design of Composite Precast Prestressed Concrete Sandwich Panels with NU-Tie." Final report. University of Nebraska–Lincoln.

11. Naito, C., J. Hoemann, M. Beacraft, and B. Bewick. 2012. "Performance and Characterization of Shear Ties for Use in Insulated Precast Concrete Sandwich Wall Panels." *Journal of Structural Engineering* 138 (1): 52–61.

12. Woltman, G., D. Tomlinson, and A. Fam. 2013. "Investigation of Various GFRP Shear Connectors for Insulated Precast Concrete Sandwich Wall Panels." *Journal of Composites for Construction* 17 (5): 711–721.

13. Frankl, B. 2008. "Structural Behavior of Insulated Precast Prestressed Concrete Sandwich Panels Reinforced with CFRP Grid." MSc thesis, Department of Civil, Construction and Environmental Engineering, North Carolina State University, Raleigh, NC.

14. Frankl, B. A., G. W. Lucier, T. K. Hassan, and S. H. Rizkalla. 2011. "Behavior of Precast, Prestressed Concrete Sandwich Wall Panels Reinforced with CFRP Shear Grid." *PCI Journal* 56 (2): 42–54.

15. Hassan, T. K., and S. H. Rizkalla. 2010. "Analysis and Design Guidelines of Precast, Prestressed Concrete, Composite Load-Bearing Sandwich Wall Panels Reinforced with CFRP Grid." *PCI Journal* 55 (2): 147–162.

16. Bunn, W. G. 2011. "CFRP Grid/Rigid Foam Shear Transfer Mechanism for Precast, Prestressed Concrete Sandwich Wall Panels." MSc thesis, Department of Civil, Construction and Environmental Engineering, North Carolina State University, Raleigh, NC.

17. Sopal, G. J. 2013. "Use of CFRP Grid as Shear Transfer Mechanism for Precast Concrete Sandwich Wall Panels." PhD diss., Department of Civil, Construction and Environmental Engineering, North Carolina State University, Raleigh, NC.

18. Hodicky, K., G. Sopal, S. Rizkalla, T. Hulin, and H. Stang. 2015. "Experimental and Numerical Investigation of the FRP Shear Mechanism for Concrete Sandwich Panels." *Journal of Composites for Construction* 19 (5): 04014083.

19. Kazem, H., W. G. Bunn, H. M. Seliem, S. H. Rizkalla, and H. Gleich. 2015. "Durability and Long Term Behavior of FRP/Foam Shear Transfer Mechanism for Concrete Sandwich Panels." *Construction and Building Materials* 98: 722–734.

20. Olsen, J. T., and M. Maguire. "Shear Testing of Precast Concrete Sandwich Wall Panel Composite Shear Connectors." in *The PCI Convention and National Bridge Conference: Proceedings, March 3–6, 2016, Nashville, Tennessee*. Chicago, IL: PCI.

21. Dutta, D., A. Jawdhari, and A. Fam. 2020. “A New Studded Precast Concrete Sandwich Wall with Embedded Glass-Fiber-Reinforced Polymer Channel Sections: Part 1, Experimental Study.” *PCI Journal* 65 (3): 78–99.

22. Jawdhari, A., and A. Fam. 2020. “A New Studded Precast Concrete Sandwich Wall with Embedded Glass-Fiber-Reinforced Polymer Channel Sections: Part 2, Finite Element Analysis and Parametric Studies.” *PCI Journal* 65 (4): 51–70.

23. ASCE (American Society of Civil Engineers). 2017. *Minimum Design Loads for Buildings and Other Structures*. ASCE/SEI 7-16. Reston, VA: ASCE.

24. ICC-ES (International Code Council Evaluation Service). 2017. “C-Grid Shear Connectors.” Report ESR-2953. Brea, CA: ICC-ES.

About the authors

Mohamed K. Nafadi, PhD, is an assistant professor of structural engineering at Assiut University in Assiut, Egypt. He is a former visiting assistant professor at the Department of Civil, Construction, and Environmental Engineering at North Carolina State University (NCSU) in Raleigh.

Gregory Lucier, PhD, is a research associate professor in the Department of Civil, Construction, and Environmental Engineering and manager of the Constructed Facilities Laboratory at NCSU.

Tugce Sevil Yaman, PhD, is an assistant professor of structural engineering at Mersin University in Mersin, Turkey. She is a former postdoctoral fellow in the Department of Civil, Construction, and Environmental Engineering at NCSU.

Harry Gleich, PE, FPCI, FACI, is the vice president of engineering for Metromont Corp. in Greenville, S.C. He is the chair of the PCI Technical Activities Council, chair of the PCI Research and Development Council, and past chair of the PCI Precast Insulated Wall Panels Committee. He is also the former chair of ACI Committee 533, Precast Panels, and former chair of ACI Committee 550, Precast Concrete Structures.

Sami Rizkalla, PhD, FPCI, FACI, FASCE, FIIFC, FEIC, FCSCE, is a Distinguished Professor Emeritus in the Department of Civil, Construction, and Environmental Engineering at NCSU.

Abstract

This paper documents the testing of six 20 ft × 4 ft × 8 in. (6.1 m × 1.2 m × 203.2 mm) precast, prestressed concrete sandwich panels constructed with continuous rigid insulation and a carbon-fiber-reinforced polymer grid shear transfer mechanism. All panels were identical except for foam type and were cast together on the same prestressing bed. Three of the six panels were fabricated with expanded polystyrene (EPS) foam insulation, and the remaining three panels were fabricated using sandblasted extruded polystyrene (XPS) foam. For each group of three panels, one was tested to failure as a control and two others were cycled 2 million times to 45% of their design ultimate load before failure testing. The tested EPS panels all failed when the applied lateral load was greater than or equal to 100 lb/ft^2 (4.79 kPa), which is 2.35 times their design load of 42.5 lb/ft^2 (2.03 kPa). The tested XPS panels all failed at the equivalent of 175 lb/ft^2 (8.38 kPa) of applied lateral pressure, which is more than 4.0 times their design load of 42.5 lb/ft^2. All four panels subjected to fatigue survived 2 million reverse-cyclic lateral load cycles without any visible signs of degradation.

https://doi.org/10.15554/pcij66.5-01

Keywords

Carbon-fiber-reinforced polymer grid, composite action, concrete wythe, fatigue, sandwich panel.

Review policy

This paper was reviewed in accordance with the Precast/Prestressed Concrete Institute's peer-review process.

Reader comments

Please address any reader comments to *PCI Journal* editor-in-chief Tom Klemens at tklemens@pci.org or Precast/Prestressed Concrete Institute, c/o *PCI Journal*, 8770 W. Bryn Mawr Ave., Suite 1150, Chicago, IL 60631.